Motion Correction in Dynamic Contrast-Enhanced Magnetic Resonance Images Using Pharmacokinetic Modeling

Mia Mojica and Mehran Ebrahimi

Faculty of Science, University of Ontario Institute of Technology, Oshawa, ON, Canada

ABSTRACT

Pharmacokinetic modeling is a mathematical modeling technique that examines the dynamics of concentration curves to reveal information about tissue microvasculature. Typically, image registration is performed as a pre-processing step to remove motion in dynamic contrast-enhanced (DCE) image sequences and ensure accurate pharmacokinetic analysis.

In this work, we introduce a registration method for correcting motion in a sequence of DCE images. The proposed method involves the use of Tofts pharmacokinetic model to generate a sequence of reference images. These images simplify the challenging task of registering DCE images by pairing each frame in the motion-corrupted sequence with a reference image that resembles the overall contrast enhancement of the template.

Abdominal DCE-MR images were used for validation. Reduction of motion in the registered sequence was observed both visually and quantitatively. Both global and local measures of registration accuracy obtained from the registered sequence and its associated signal intensity curves were smaller than their pre-registration counterparts.

Keywords: image registration, pharmacokinetic modeling, Tofts model, elastic registration

1. INTRODUCTION

Dynamic contrast-enhanced (DCE) imaging is a technique where a sequence of images are acquired before and after the administration of a paramagnetic contrast agent. DCE protocols can be readily incorporated into existing CT and MRI protocols [1].

The concentration curves resulting from the temporal enhancement pattern of a tissue enable the analysis of the tissue microvasculature, which in turn can be used in tumour diagnosis. It has been shown that the micro-circulatory parameters that can be derived from the analysis of concentration curves can be used to characterize the malignancy of a tumour, aid in identifying appropriate courses of treatment and in assessing a patient's response and resistance to treatment.[2,3]

Image registration is typically performed as a pre-processing step to reduce motion in a sequence of DCE-MR images prior to the analysis of tissue concentration curves. However, the absorption of the contrast medium into the region of interest creates intensity variations in the image sequence, thereby complicating the alignment of structural information in DCE images.

Some workarounds to the challenges introduced by intensity variations in contrast-enhanced images involved the use of surface markers and optical motion tracking devices to correct misalignment in image pairs, as in [4]. Others proposed the construction of a set of synthetic images to assist in the registration of images. For instance, in [5], the registration problem was divided into sub-problems using auxiliary images computed from the conditional probability distribution of image voxel pairs. These auxiliary images were registered to the original images using the Sum of Squared Distances (SSD) distance measure measure. In [6], a general tracer-kinetic model described by an input response function convolved with the plasma input function was used to obtain

Further author information: (Send correspondence to)
Mia Mojica: E-mail: Mia.Mojica@uoit.ca
Mehran Ebrahimi: E-mail: Mehran.Ebrahimi@uoit.ca

Medical Imaging 2021: Image Processing, edited by Ivana Išgum, Bennett A. Landman, Proc. of SPIE Vol. 11596, 115962S · © 2021 SPIE · CCC code: 1605-7422/21/$21 · doi: 10.1117/12.2580973

time-activity curves. These curves were then used to assist a succeeding groupwise registration framework based on an Expectation-Maximization framework.[7]

In this work, we present a pharmacokinetic (PK) approach for correcting motion in a DCE sequence. It employs a pharmacokinetic model for the uptake of the contrast agent to generate a sequence of reference images, which then allows for the implementation of a simple elastic registration method coupled with the SSD.

2. DATA

A sequence of abdominal MR images was used in our experiments. The scans were acquired with a T1-weighted fast spoiled gradient-echo (FSPGR)[8] sequence. Spatial resolution was 1.88mm by 1.88mm by 8mm in the superior/inferior (S/I), left/right (L/R), and anterior/posterior (A/P) directions respectively. Temporal resolution was approximately 3.7 seconds per volume as in [3, 9, 10].

3. METHODS

In this section, we discuss the components that are vital in generating the synthetic images that would simplify the motion correction problem in DCE sequences, namely the Tofts pharmacokinetic model for contrast uptake and the Levenberg-Marquardt Algorithm (LMA) for non-linear least squares minimization.

3.1 Tofts Pharmacokinetic Model

The Tofts pharmacokinetic model,[11,12] proposed by Tofts and Kermode, is frequently used to characterize contrast dynamics in tumours.[13] The tissue concentration of Gd-DTPA is described by the biexponential function

$$C(t) = DK^{\text{trans}} \sum_{i=1}^{2} a_i \left[\frac{\exp\left(-k_{\text{ep}} t\right) - \exp\left(m_i t\right)}{m_i - k_{\text{ep}}} \right], \tag{1}$$

where D is the injected dose of the contrast agent, K^{trans} the influx volume transfer constant, K_{ep} the efflux rate constant from the extravascular-extracellular space (EES) to plasma, the m_i's are the rate constants of CA clearance, and the a_i's are the corresponding amplitudes. In this model, equilibrium of the injected contrast agent between the plasma and EES (i.e., the whole body) and the isodirectional permeability of the plasma and EES compartments are assumed.[11,14] The schematics of the Tofts model are provided in Figure 1.

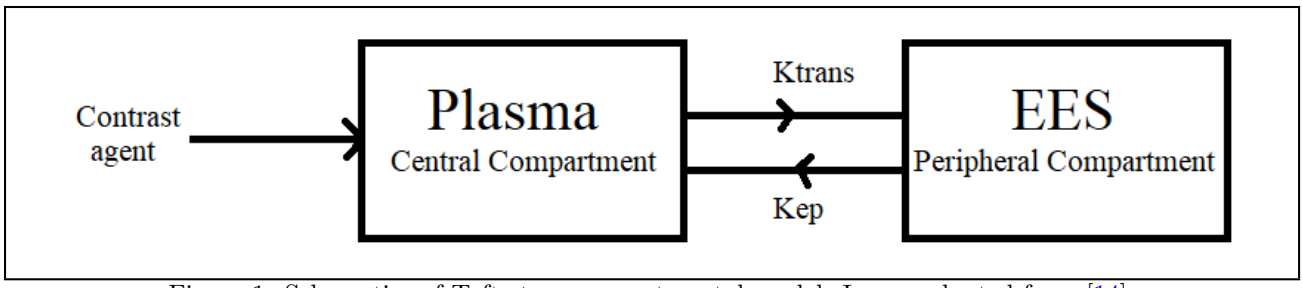

Figure 1: Schematics of Tofts two-compartmental model. Image adapted from [14].

3.2 Levenberg-Marquardt Algorithm

In practice, signal intensity curves (SI) from a sequence of DCE images are fitted to one of the pharmacokinetic models using a nonlinear fitting method like the Levenberg-Marquardt algorithm (LMA).[15] The LMA is an iterative procedure for minimization that uses first-order information to approximate the optimal solution.

Suppose we are given a set of data points (x_i, y_i), $i = 1, \ldots, n$, and we want to find the parameter α^* of the curve $f(x, \alpha^*)$ that minimizes the sum of squared residuals

$$L(\alpha) = \sum_{i=1}^{n} \left[y_i - f(x_i, \alpha) \right]^2 . \tag{2}$$

Using the first-order Taylor expansion of the function f around α and letting $J_i = \partial f(x_i, \alpha)/\partial\alpha$, an approximation for the sum of squared residuals at the new estimate $\alpha + \delta$ can be computed as

$$L(\alpha + \delta) = \sum_{i=1}^{n} \left[y_i - f(x_i, \alpha) - J_i \delta \right]^2 . \tag{3}$$

Modifying the normal equation of (3) to include a damping factor $\lambda \geq 0$ for diagonal elements of the symmetric matrix $J^T J$ yields

$$\delta = \left[J^T J + \lambda \, \mathrm{diag}(J^T J) \right]^{-1} \left[J^T \left[y - f(\alpha) \right] \right].$$

3.3 Sequence of Synthetic Reference Images

To facilitate the construction of a motionless sequence of reference images, we plotted the intensity of every pixel in the image domain at every discrete time step t_i in the image acquisition process and fitted each pre-registration SI curve to the Tofts model via the Levenberg-Marquardt algorithm. Subsequently, predictions of the intensity value of every pixel at every time step were given by the points on the best-fit curves, which in turn allowed us to construct the synthetic reference sequence. See Figures 2-3.

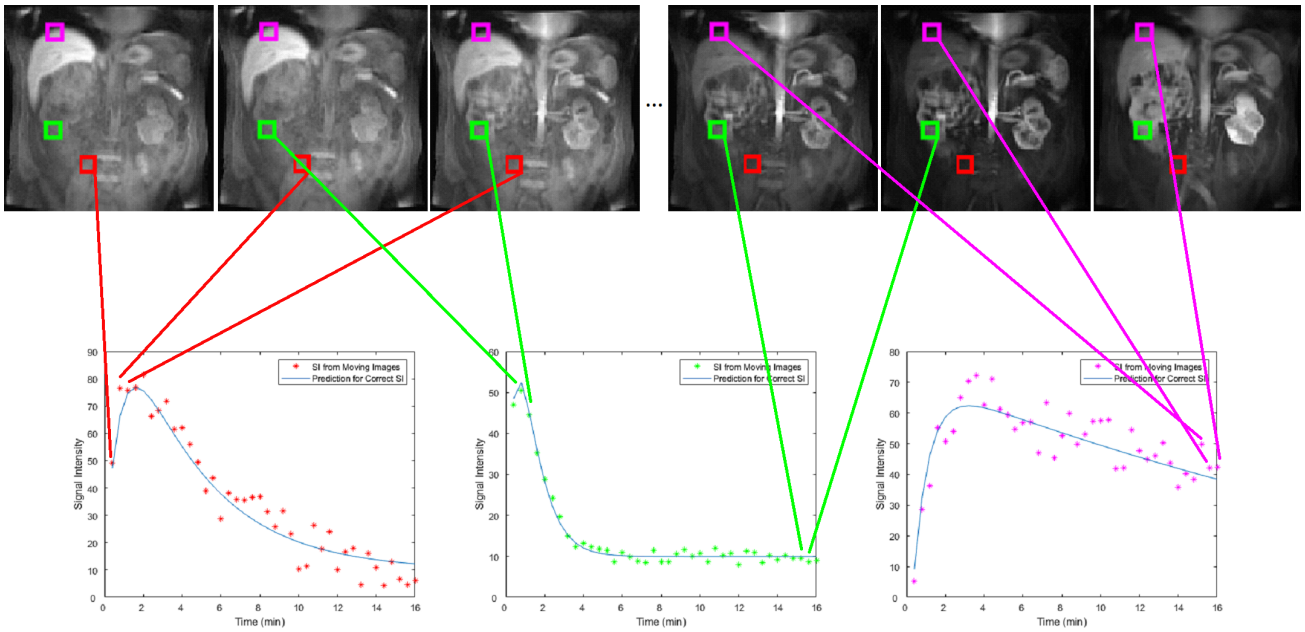

Figure 2: The best-fit prediction curves were obtained after computing the microcirculatory parameters that minimize the sum of squared residuals between the pre-registration SI curves and the Tofts model. The points on a prediction curve represents the projected intensities of a pixel at different time steps in the image acquisition process.

3.4 Elastic Registration

Given the i^{th} frame $\mathcal{T}_i$ of a DCE sequence, we want to find a transformation θ_i that aligns $\mathcal{T}_i$ to its corresponding synthetic reference image $\mathcal{R}_i$. That is, we aim to solve the optimization problem

$$\theta_i = \underset{\theta}{\mathrm{argmin}} \; \mathcal{D}^{\mathrm{SSD}} \left[\mathcal{R}_i, \mathcal{T}_i \left[\theta(x) \right] \right] + \alpha \mathcal{S} \left[\theta(x) \right],$$

where

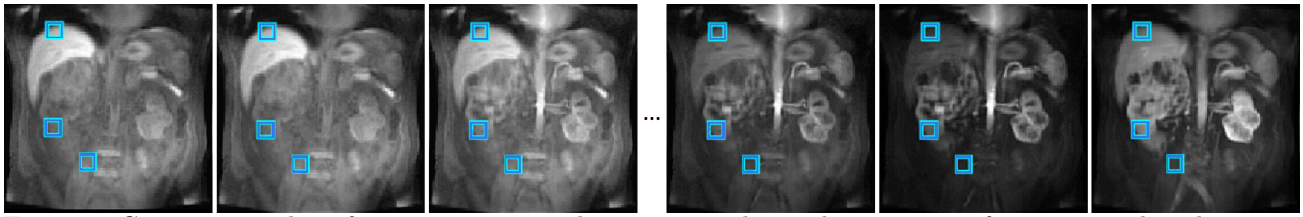

Figure 3: Constructing the reference images entails generating the prediction curves for every pixel in the image domain. The intensity value of a pixel x in the i^{th} reference image is given by the point $P^x(t_i)$ on the prediction curve associated with x.

- $\mathcal{T}_i\left[\theta(x)\right]$ is a transformed version of the template image $\mathcal{T}_i$,
- $\mathcal{D}^{\text{SSD}}\left[\mathcal{R}_i, \mathcal{T}_i\left[\theta(x)\right]\right]$ denotes the Sum of Squared Distances between the reference and transformed template, and
- $\mathcal{S}\left[\theta(x)\right]$ is the elastic regularization term[16] that controls the amount of local deformations.

4. EXPERIMENTS AND RESULTS

The proposed pharmacokinetic method was validated on the DCE-MR sequence of abdominal images described in Section 2.

Following the construction of the reference images as discussed in Section 3.3, elastic registration was implemented to align each frame in the initial motion-corrupted DCE sequence to its corresponding reference. The final set of registered images corresponds to the motion-corrected sequence from the proposed method.

Shown in Figure 4a are the absolute difference images between some successive frames in the motion-corrupted sequence. Prior to registration, the difference images were influenced by both diaphragm motion and the wash-in of the contrast agent. After aligning the template images to their corresponding synthetic references – some of which are displayed in Figure 4b – the difference images (Figure 4d) between consecutive PK-registered images in Figure 4c were mostly null, except for the regions that were enhanced by the contrast agent.

To quantify the amount of remaining motion in the registered sequence, we computed the target registration error (TRE), as well as the mean squared error (MSE) and coefficient of variation (CV) of the SI curves before and after PK registration. TREs denote the distances of specified gridpoints in the template images from their correct location in the ground truth. Meanwhile, MSEs quantify how close the SI curves of the final registered images are to the SI curves of the ground truth sequence. Finally, CVs measure the smoothness of the SI curves.

With respect to the initial DCE sequence, the proposed method yielded smaller post-registration average TREs, which means that the transformed template grid resembles the reference grid more closely after performing PK registration. Post-registration MSE and CV were also lower than their pre-registration counterparts. These imply that the proposed method produced smoother SI curves with smaller fluctuations, which then translates to more accurate local alignments.

5. CONCLUSIONS

Here, we introduced a registration pipeline that employs Tofts pharmacokinetic model to generate synthetic reference images for every frame in a DCE sequence. Doing so simplified the problem of eliminating naturally occurring motion from a sequence of DCE images by enabling the use of a simple elastic registration algorithm coupled with the SSD distance metric. This is a departure from registration methods that require the inclusion of an intensity correction term to properly align DCE images [3, 9, 17, 18].

Reduction of motion in the registered sequence was observed both visually and quantitatively. In terms of both global and local measures of accuracy, the TRE, CV, and MSE of SI curves resulting from the proposed pharmarcokinetic method were all significantly lower than their pre-registration counterparts.

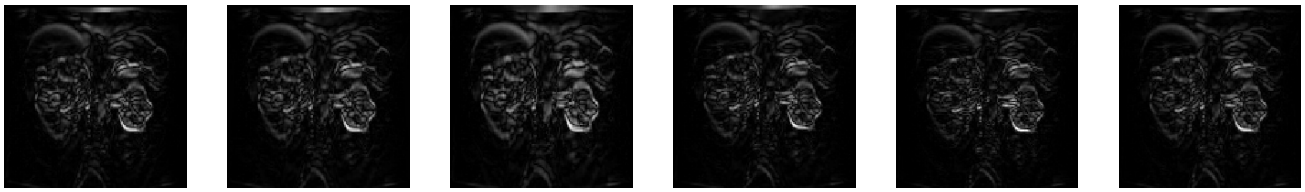

(a) Absolute difference between some consecutive images in the motion-corrupted sequence

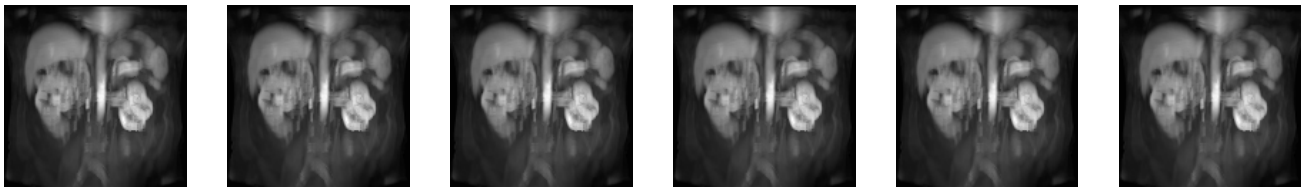

(b) Some of the generated reference images

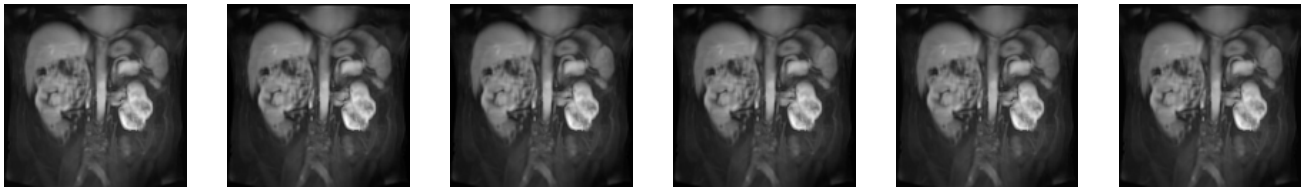

(c) Some consecutive registered images in the sequence

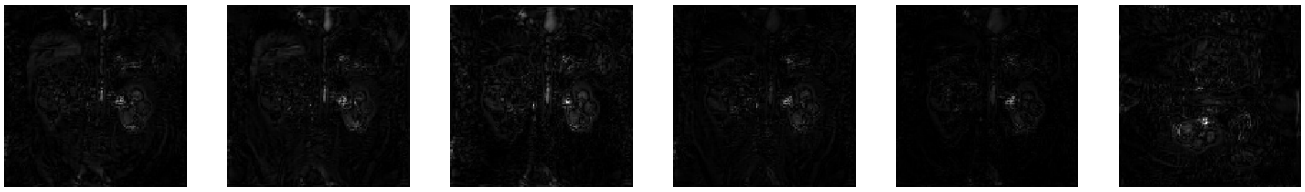

(d) Absolute difference between some consecutive images in the registered sequence

Figure 4: Results of the registration of the sequence of DCE images to the motionless sequence of synthetic reference images. (a) Difference images $|\mathcal{T}_i - \mathcal{T}_{i-1}|$ from some consecutive frames in the DCE sequence with motion, (b) consecutive synthetic reference images, (c) some consecutive registered images $\mathcal{T}_i[\theta_i]$, and (d) difference images $|\mathcal{T}_i[\theta_i] - \mathcal{T}_{i-1}[\theta_{i-1}]|$ between consecutive frames in the motionless registered sequence.

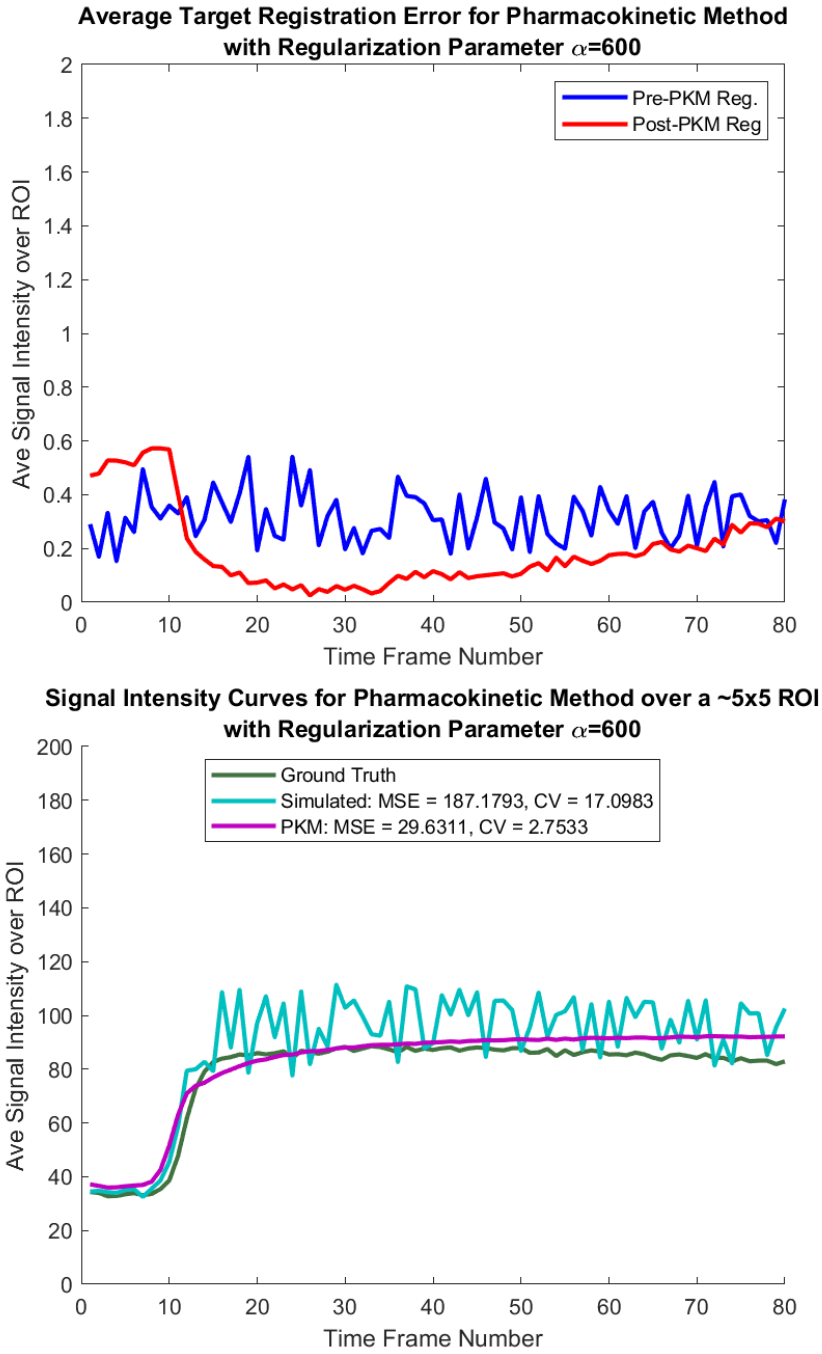

Figure 5: Frame-by-frame average TRE and SI curves for $\alpha = 600$. The location of the gridpoints in the template images were tracked in the sequence of motion-corrupted (pre-registration) and motion-corrected images. The TREs are the distances of these points from their correct location in the ground truth/motionless dataset.

ACKNOWLEDGMENTS

This work was supported in part by an NSERC Discovery Development Grant for Mehran Ebrahimi. Mia Mojica was supported by a Doctoral Ontario Trillium Scholarship (OTS). The authors would also like to acknowledge Dr. Anne Martel of Sunnybrook Research Institute for providing the DCE-MRI data.

REFERENCES

[1] O'Connor, J., Tofts, P., Miles, K., Parkes, L., Thompson, G., and Jackson, A., "Dynamic contrast-enhanced imaging techniques: CT and MRI," *The British journal of radiology* **84**(special_issue_2), S112–S120 (2011).

[2] Dickie, B. R., Rose, C. J., Kershaw, L. E., Withey, S. B., Carrington, B. M., Davidson, S. E., Hutchison, G., and West, C. M., "The prognostic value of dynamic contrast-enhanced MRI contrast agent transfer constant Ktrans in cervical cancer is explained by plasma flow rather than vessel permeability," *British journal of cancer* **116**(11), 1436 (2017).

[3] Lausch, A., Ebrahimi, M., and Martel, A., "Image registration for abdominal dynamic contrast-enhanced magnetic resonance images," IEEE.

[4] Koshino, K., Watabe, H., Hasegawa, S., Hayashi, T., Hatazawa, J., and Iida, H., "Development of motion correction technique for cardiac 15 o-water pet study using an optical motion tracking system," *Annals of nuclear medicine* **24**(1), 1–11 (2010).

[5] Sun, Y., Yan, C. H., Ong, S.-H., Tan, E. T., and Wang, S.-C., "Intensity-based volumetric registration of contrast-enhanced MR breast images," in [*International Conference on Medical Image Computing and Computer-Assisted Intervention*], 671–678, Springer (2006).

[6] Jiao, J., Searle, G. E., Tziortzi, A. C., Salinas, C. A., Gunn, R. N., and Schnabel, J. A., "Spatial-temporal pharmacokinetic model based registration of 4d brain pet data," in [*International Workshop on Spatio-temporal Image Analysis for Longitudinal and Time-Series Image Data*], 100–112, Springer (2012).

[7] Moon, T. K., "The expectation-maximization algorithm," *IEEE Signal processing magazine* **13**(6), 47–60 (1996).

[8] Chavhan, G. B., Babyn, P. S., Jankharia, B. G., Cheng, H.-L. M., and Shroff, M. M., "Steady-state mr imaging sequences: physics, classification, and clinical applications," *Radiographics* **28**(4), 1147–1160 (2008).

[9] Lausch, A., *Nonrigid registration of dynamic contrast-enhanced MRI data using motion informed intensity corrections*, PhD thesis (2011).

[10] Mojica, M. and Ebrahimi, M., "An unbiased groupwise registration algorithm for correcting motion in dynamic contrast-enhanced magnetic resonance images," in [*Image Analysis for Moving Organ, Breast, and Thoracic Images*], 42–52, Springer (2018).

[11] Tofts, P. S. and Kermode, A. G., "Measurement of the blood-brain barrier permeability and leakage space using dynamic MR imaging," *Magnetic resonance in medicine* .

[12] Tofts, P., "T1-weighted DCE imaging concepts: Modelling, acquisition and analysis," *MAGNETOM Flash* (2010).

[13] Martel, A. L., "A fast method of generating pharmacokinetic maps from dynamic contrast-enhanced images of the breast," in [*International Conference on Medical Image Computing and Computer-Assisted Intervention*], 101–108, Springer (2006).

[14] Chikui, T., Obara, M., Simonetti, A. W., Ohga, M., Koga, S., Kawano, S., Matsuo, Y., Kamintani, T., Shiraishi, T., Kitamoto, E., et al., "The principal of dynamic contrast enhanced MRI, the method of pharmacokinetic analysis, and its application in the head and neck region," *International journal of dentistry* **2012** (2012).

[15] Gavin, H., "The Levenberg-Marquardt algorithm for nonlinear least squares curve-fitting problems," (2019).

[16] Modersitzki, J., [*FAIR: Flexible algorithms for image registration*], SIAM (2009).

[17] Aghajani, Khadijeh, e. a., "A robust image registration method based on TV regularization under complex illumination changes," *CMPB* .

[18] Ebrahimi, M. and Martel, A., "A general PDE-framework for registration of contrast enhanced images," in [*International Conference on Medical Image Computing and Computer-Assisted Intervention*], 811–819, Springer (2009).

[19] Tofts, P. S., "Modeling tracer kinetics in dynamic Gd-DTPA MR imaging," *Journal of magnetic resonance imaging* **7**(1), 91–101 (1997).

[20] Tofts, P. S., Berkowitz, B., and Schnall, M. D., "Quantitative analysis of dynamic Gd-DTPA enhancement in breast tumors using a permeability model," *Magnetic resonance in medicine* **33**(4), 564–568 (1995).